Volume 1
Number 5
1 September 2024
Pages 823–1095

RSC Applied Interfaces

rsc.li/RSCApplInter

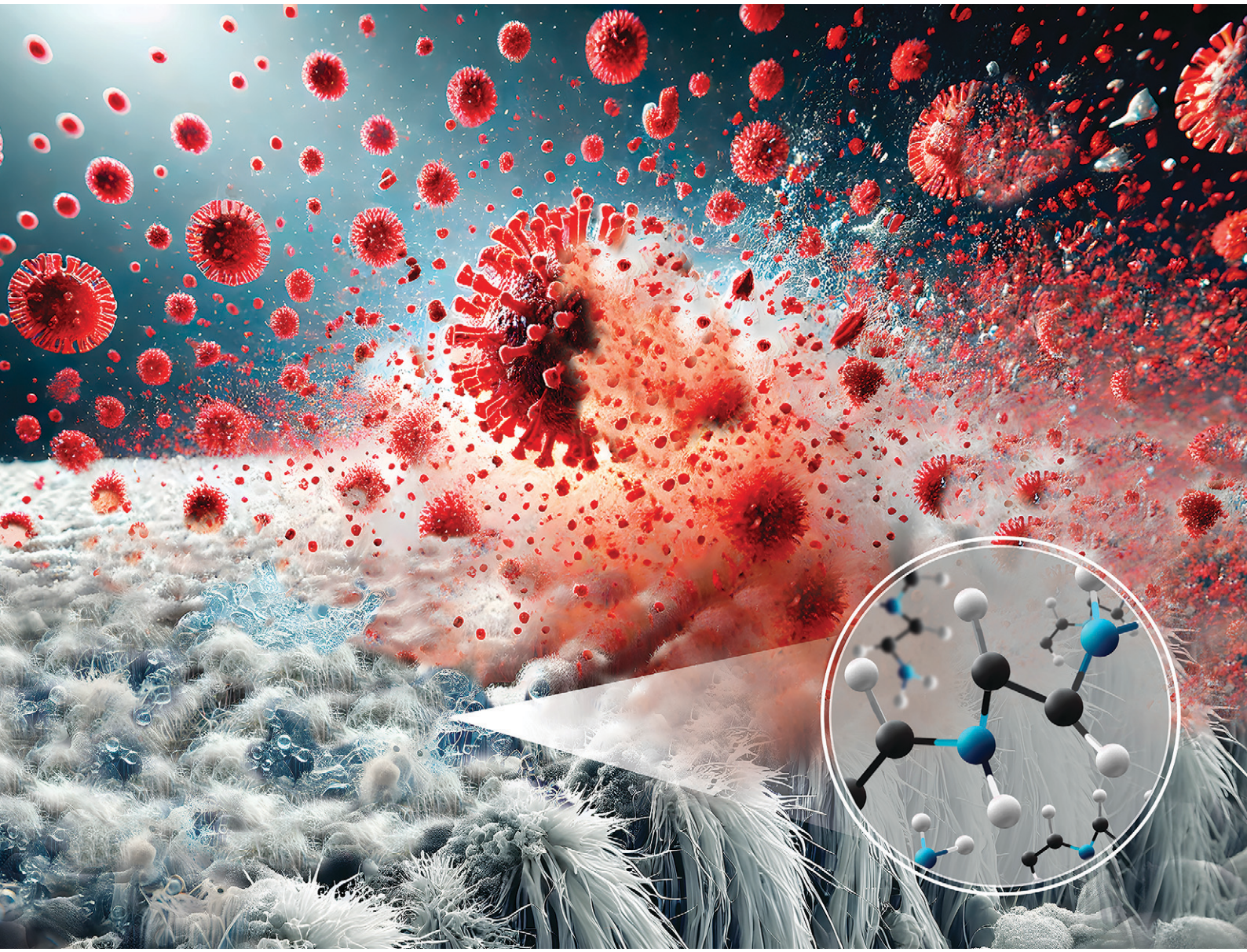

ISSN 2755-3701

ROYAL SOCIETY OF CHEMISTRY

PAPER

Pascal Y. Vuillaume *et al.*

Polypropylene fabric coated with branched polyethyleneimine derivatives for high antiviral activity

RSC Applied Interfaces

ROYAL SOCIETY OF CHEMISTRY

PAPER

View Article Online
View Journal | View Issue

Cite this: *RSC Appl. Interfaces*, 2024, 1, 908

Polypropylene fabric coated with branched polyethyleneimine derivatives for high antiviral activity†

Lori Leblond,[a] Abdessadk Anagri,[a] Jacques Fiset,[a] Marie-Yolande Borget,[b] Philippe Bébin,[a] Nancy Dumais[b] and Pascal Y. Vuillaume *[a]

Due to the COVID-19 pandemic context, the demand for new materials with antiviral and antibacterial properties has been increasing in recent years following an awareness to help prevent future outbreaks. However, current material approaches based on metal ions, metal particles, chlorine-based disinfectants, and polymer nanocomposites cause environmental and health risks. Herein, we report a one-step low-cost process of a highly effective antiviral surface coating of polyethylenimine (PEI) and alkylated PEI derivatives (*N*-hexyl-PEI and *N*-hexyl,*N*-methyl-PEI) on a filtration felt made of polypropylene fibers. Results based on a comparison of the antiviral efficiency of PEI and alkylated PEI derivatives by exposure to feline calicivirus (FCV) are presented. Chemical composition and features of the surface morphology of coatings were characterized by ^{1}H-NMR spectroscopy, Fourier transform infrared spectroscopy (FTIR), X-ray photoelectron spectroscopy (XPS), scanning electron microscopy (SEM) and energy-dispersive spectrometry (EDS). The antiviral activity of PEI and PEI alkylated derivatives coated on PP felt at three different concentrations was evaluated. The results showed a stronger effective inactivation of FCV for the PEI-coated felt with a reduced viral titer from ≥99.9% for the non-coated felt to ≥99.9999% for the PEI-coated felt, after 4 hours, which represents a 6 $\log_{10}$ (CFU mL^{-1}) reduction of viruses. Moreover, the cytotoxicity of *N*-hexyl,*N*-methyl-PEI which contains more quaternary ammonium functions did not inhibit the viability of Crandell-Rees feline kidney (CRFK) cell culture.

Received 25th April 2024,
Accepted 16th June 2024

DOI: 10.1039/d4lf00142g

rsc.li/RSCApplInter

1. Introduction

SARS-CoV-2 has infected over 772 million people globally, causing almost 7 million deaths as of November 2023.[1] It primarily spreads through infectious aerosol when people come in contact within two meters of each other. While enclosed spaces increase the risk of transmission. The virus can also be transmitted indirectly through contact with contaminated surfaces. To reduce the spread of SARS-CoV-2 measures such as physical distancing, wearing protective masks, and sanitizing surfaces are recommended by WHO and governments.

However, personal protective equipment such as masks do not completely mitigate the risk of contagion because they do not inactivate the viral particles and do not prevent their proliferation. The demand for high-performance materials with the capability of annihilating bacteria and viruses has significantly increased since the beginning of the COVID-19 pandemic. Hydroalcoholic gels, metal ions, and nanoparticles (constitute of *e.g.*, silver and copper), polymer nanocomposites made of graphene or carbon nanotubes, disinfectants of chlorine derivatives such as hypochlorite, chlorine dioxide, triclosan, chlorhexidine, tributyltin and finally ozone are common biocides reported in the literature.[2–10] Although their biocidal properties are quite effective, these compounds have major disadvantages due to their short duration of action caused by rapid leaching. This leach-out is a hazard to the environment because they are mostly toxic.[6,7] In addition, over the long term, the misapplication of these disinfectants can lead to the development of bacterial resistance.[3,7]

Ultraviolet (UV) radiation is also a widely used water and surface disinfection technology to inactivate microorganisms. Following the exposure and absorption of UV radiation, the nucleotides composing DNA and RNA are damaged and the process of cell reproduction is blocked.[11] Nevertheless, this disinfection method carries a risk of cell regrowth of

[a] *COALIA, Thetford Mines, Quebec, G6G 1N1, Canada.*
E-mail: pvuillaume@coalia.ca
[b] *Department of Biology, University of Sherbrooke, Sherbrooke, Quebec, J1K 2R1, Canada*

† Electronic supplementary information (ESI) available. See DOI: https://doi.org/10.1039/d4lf00142g

microorganisms by photoreactivation. After treatment by UV, cells can repair if the dose of irradiation is not powerful enough.[12]

Quaternary ammonium salts are known effective in rupturing Gram-negative and Gram-positive bacteria cell membranes. They can thus confer antibacterial properties to polymers when they are incorporated therein.[13] Amine functional groups on a polymer's backbone can also be chemically modified into quaternary ammonium. Those polymers are referred to as polyquaternary ammonium and widely as polycations. Laschewsky *et al.* synthesized many charged polymers including polycations and reported that those having quaternary ammonium functions present a well-known bactericidal activity.[14] Some polycations are functionalized macromolecules with permanent positively charged groups attached to the chains while others are not fully charged because they are partially dissociated in solution and strongly depend on the pH.[15]

Antimicrobial and antibacterial properties of polycations, such as quaternary ammonium compounds (QACs), have been widely demonstrated.[16–19] Numerous studies report on the biocidal activity of QACs coated on polymers-based fabrics, in particular polypropylene (PP) surfaces. Kumaran *et al.* demonstrated that QAC-based antimicrobial coatings could be easily applied to various mask fabrics, rapidly inactivating multiple viruses and bacteria.[20] Sorci *et al.* applied ultrathin QAC coatings to N95 respirator masks using UV grafting, maintaining filtration efficiency and providing broad-spectrum antiviral activity.[21] Furthermore, Hirao *et al.* developed a method for three-dimensionally surface-grafting poly(*N*-benzyl-4-vinylpyridinium bromide) onto PP, achieving durable antiviral coatings resistant to abrasion by optimizing UV-induced polymerization.[22] The antibacterial action mechanism of QACs is mainly explained by the electrostatic and hydrophobic interactions existing between the positively charged polymer (N^+) and the negatively charged cell membrane of bacteria when they are close to each other.[3,6,23] The polycation captures the surrounding bacteria through electrostatic attraction and adsorbs onto the bacteria cell wall's surface.[5,24] The hydrophobic alkyl chains of the polymer penetrate the phospholipid membrane and rupture it.[16,25,26] Cellular permeability is disrupted and cytolytic damage causes intracellular fluid and its cytoplasmic constituents such as potassium ions, DNA, and RNA to leak out.[2,5,27] It results in the immediate death of the organism and the bacterial cell reproduction is thereby inhibited.[2,5,13] During the adsorption of QACs to the bacteria's surface, an additional inactivation process is discussed in literature.[16,23] A cation exchange within the cytoplasmic membrane can also occur and destabilize the intracellular matrix. Divalent calcium and magnesium cations, essential for neutralizing membrane components, become free to diffuse out through the cell wall by ion exchange.[13] The exchange of these structural cations causes a loss of membrane integrity and inactivates the bacteria. The antibacterial activity of QACs depends therefore on the surface N^+ charge density.[3] However, a high amount of positive charges present on the polycation weakens its hydrophobic character responsible for the membrane rupture.[6] Thus, a balance between N^+ charge density and hydrophobicity is imperative. The annihilating efficacy is strongly linked to the length of the hydrophobic alkyl chains.[16] It has been demonstrated using the zeta potential that the QACs with long carbon chains have superior biocidal properties compared to those with shorter chains.[12,13] The optimal chain length of alkyl based on literature ranges from six to eight carbons. This length represents a compromise between N^+ charge density and hydrophobicity both useful for the pathogen inactivation mechanism.[3] Hexyl and octyl chains are more efficient to disrupt the cytoplasmic membrane compared to methyl chain groups.

The annihilation mechanism of QACs prevents bacterial resistance and does not involve oxidative reactions and the formation of disinfection by-products in the water.[3,28] Furthermore, the use and the development of these polymers are interesting due to their non-volatility, chemical stability, difficulty in penetrating the skin and their long-term biocidal activity.[13] Alkoxysilanes, exchange resins, ionenes, soluble and insoluble pyridinium-type polymers are only a few examples of cationic materials frequently used to eliminate pathogens.[16]

Several articles mentioned that the annihilating mechanisms of QACs applied to enveloped viruses such as coronaviruses due to the favorable electrostatic and hydrophobic interactions between the QACs' functional groups and the amino acid residues of reverse transcriptase involved in the viral cycle.[29–31] The virions can be damaged by the alkyl chains and the interior of the nucleocapsid is released causing the inactivation of the viruses.[13,23,21,32] The virucidal action of alkylated PEI derivatives has been demonstrated on the influenza A, the most infectious type in humans, hence the hypothesis of their potential efficiency in inactivating SARS-CoV-2.[25]

Due to their mentioned benefits, PEI and its derivatives have been therefore targeted for a potential antiviral activity against COVID-19. In this study, alkylated PEI derivatives were synthesized and applied with the aim of developing a virucidal coating on a filtration felt made of polypropylene fibers employed in the manufacture of protective masks and building air filtration systems.[6,26,33] The effect of alkylation degree and the atomic concentration of positively charged nitrogen (N^+) on the antiviral activity of PEI coatings were investigated. Moreover, the non-coated felt for comparison and the coated felts were tested against feline calicivirus (FCV) as the foundation of SARS-CoV-2 according to the International Standard ISO 18184:2019,[34] which may have significant value in the development of virucidal coatings against other viruses and the prevention of possible epidemics in the future.

2. Experimental section

Chemical materials

Polypropylene fabrics with mean thickness of 1.5 mm was supplied by Alkegen (Quebec, Canada). Branched polyethylenimine (PEI) of molecular weight of 750 kDa (50% w/w aqueous solution), 1-bromohexane (≥98.0%), *tert*-amyl alcohol (TAA) (≥99.0%), potassium carbonate (≥98%), iodomethane (≥99.0%) and 2-propanol (≥99.5%), were all purchased from Sigma-Aldrich and used without further purification. Spectrapor® dialysis membranes (VWR) with a nominal cut-off of 3500 Da were used for dialysis. Water used for dialysis was purified by a Millipore Milli-Q water purification system (resistance 18.2 MΩ).

Cells, virus and reagents

Crandell-Rees feline kidney (CRFK) cell (cat kidney cell origin, ATCC CCL-94) and feline calicivirus (FCV) (ATCC VR-782) were purchased from ATCC. Eagle's minimum essential medium (EMEM) with Earle's salts, with L-glutamine was bought from Wisent Bio Products. Horse serum, 100 μg mL^{-1} penicillin G, and 100 μg mL^{-1} streptomycin were also purchased from Wisent Bio Products.

Cells culture

CRFK cells were grown in growth medium made up from EMEM supplemented with 10% heat-inactivated horse serum (HS), 1% penicillin G/streptomycin and maintained in a 5% CO_2 incubator at 37 °C up to 90% confluent monolayer. Then, the cells were washed with phosphate buffered saline (PBS), transferred to 96 wells microplate, and left to growth for an additional three days until reaching a confluent monolayer of in each well. Three columns in the microplate were assigned to each sample.

Synthesis of *N*-hexyl-PEI and *N*-hexyl,*N*-methyl-PEI

PEI modifications were accomplished according to the protocol described by Haldar *et al.*[25] Polymer's molecular weight constitutes an important factor affecting its biocidal properties.[35] We used the 750 kDa branched PEI in this study due to its superior antibacterial capacity over low molecular weight PEI.[35,36] The aqueous PEI-750 kDa solution was first dried at 110 °C in an oven under reduced pressure. Water is immiscible with reagents used as alkylating agents and must be removed to facilitate the alkylation reaction.[33] The PEI's water content was around 3 wt% after drying at 80 °C under vacuum for 2 days (see Fig. 1b). ^{1}H-NMR (400 MHz, DMSO-d_6): δ = 3.8–2.7 to 2.7–2.3 [broad, –C**H**$_2$– (a–e)]; 1.87 [s, 1H, N**H**]; 1.16 [s, 2H, N**H**$_2$] (see Fig. 1a).

N-Hexyl-PEI (PEI-H) (step 1 (see Fig. 1b)

4 mmol of dried PEI were dissolved in 25 mL of TAA in a three-neck round bottom flask equipped with a magnetic stirrer and a condenser. After homogenization of the polymer in alcohol at 60 °C, 56 mmol of potassium carbonate and 79 mmol of 1-bromohexane were added to the flask. To proceed with the hexylation reaction, the mixture was stirred and heated at 110 °C for 72 h. Dialyses were then performed several times on the recovered product in deionized water to remove excess potassium carbonate and 1-bromohexane. The

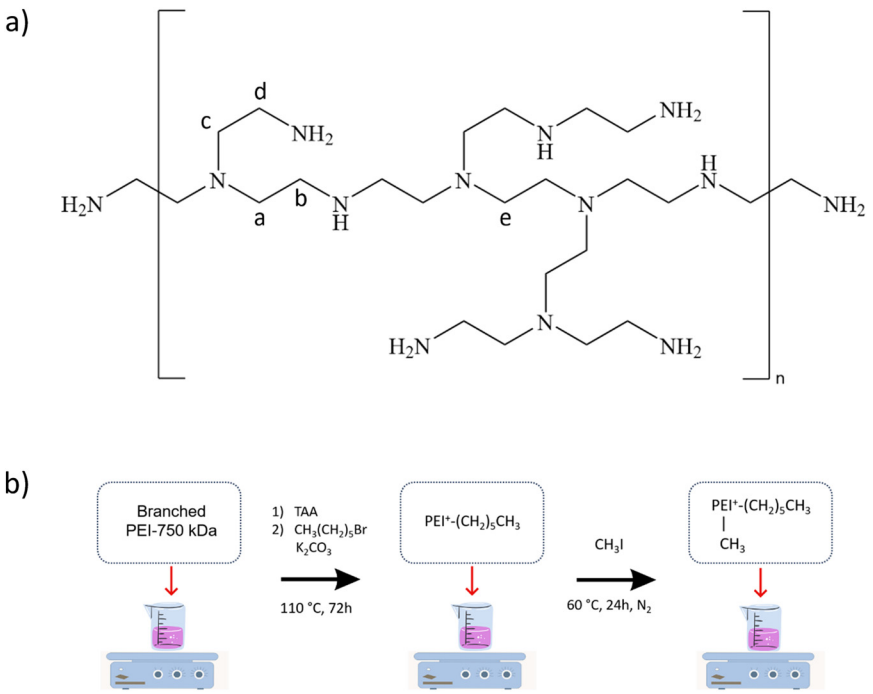

Fig. 1 (a) Chemical structure of branched PEI (750 kDa); (b) schematic route to alkylated PEIs synthesis.

content of the dialysis membrane was then dried overnight and characterized. ^{1}H-NMR (400 MHz, $CDCl_3$): δ = 4.6 [t, 2H, $-N^+-CH_2-CH_2-N^+$]; 4.2–2.7 [t, 2H, $N-CH_2-(CH_2)_4-CH_3$], [s, 3H, $-N^+-CH_3$]; 2.0–1.6 [t, 6H, $N-CH_2-CH_2-(CH_2)_3-CH_3$]; 1.6–1.1 [broad, $N-CH_2-(CH_2)_4-CH_3$]; 0.95–0.8 [t, 3H, $N-CH_2-(CH_2)_4-CH_3$].

N-Hexyl,*N*-methyl-PEI (PEI-HM) (step 2 (see Fig. 1b)

The polymer (PEI-H) recovered from the previous step (3.75 g) was dissolved in 25 mL of TAA at 60 °C using another round bottom flask equipped with a magnetic stirrer and a condenser. The flask was closed with a septum, put under inert atmosphere by introducing nitrogen, and 88 mmol of iodomethane were added to it. The mixture was then stirred and heated at 60 °C for 24 h to promote methylation. The polymer's purification was carried out using several dialysis performed in deionized water. The content of the dialysis membrane was dried overnight and characterized. ^{1}H-NMR (400 MHz, $CDCl_3$): δ = 4.5–3.9 [t, 2H, $-N^+-CH_2-CH_2-N^+$]; 3.9–2.7 [t, 2H, $N-CH_2-(CH_2)_4-CH_3$], [s, 3H, $-N^+-CH_3$]; 2.0–1.6 [t, 6H, $N-CH_2-CH_2-(CH_2)_3-CH_3$]; 1.6–1.2 [broad, $N-CH_2-(CH_2)_4-CH_3$]; 0.95–0.8 [t, 3H, $N-CH_2-(CH_2)_4-CH_3$].

Characterization of polymers

^{1}H NMR spectroscopy was achieved using an Agilent Varian 500 MHz spectrometer. The PEI spectrum was recorded in dimethyl sulfoxide-d_6 solvent and the alkylated PEI derivatives spectra were obtained in deuterated chloroform both at ambient temperature. The chemical composition of polycations was characterized by a Perkin Elmer System (Spectrum 100) equipped with an attenuated total reflectance unit. Fourier transform infrared (FTIR) spectra were recorded in the 400–3600 cm^{-1} domain with a resolution of 2 cm^{-1}. The acquisition of 16 scans was performed for each compound. In order to investigate the surface chemical composition of the polymers, X-ray photoelectron spectroscopy (XPS) analyses were performed using a Kratos Axis Ultra DLD instrument. X-ray monosource (Al Kα = 1486.6 eV) at 225 W was used to record survey and high-resolution spectra with charge neutralization. The spectra were recorded at a pass energy of 80 eV for survey spectra and 20 eV for high-resolution acquisition of core level spectra. The C–C and C–H contributions to the C 1s high-resolution for a polymer was adjusted to 285 eV to correct the charging effect since it is the most intense peak of the C1s orbital (except for the PEI which was corrected to 285.56 eV according to the high-resolution XPS of organic polymers database).[37] The analysis was performed on a 700 μm × 300 μm sampling oval area at a takeoff angle of 90°. The data was analyzed using the CasaXPS software. Background subtraction was performed according to Shirley or the linear models when necessary.

Preparation of virucidal polymeric coatings

PEI and the modified quaternary PEI derivatives were each dissolved in a solution of water and 2-propanol (40/60% v/v).

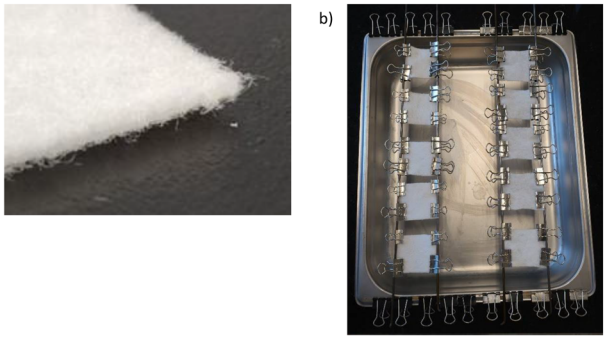

Fig. 2 (a) Image of PP fiber filtration felt and (b) assembly for the deposition of PEI and alkylated PEI derivatives at a concentration of 1 × 10^{-4} μmol N per cm^2.

These solutions were respectively diluted at five concentrations (1; 1 × 10^{-1}; 1 × 10^{-2}; 1 × 10^{-3} and 1 × 10^{-4} μmol N per cm^2). A commercial filtration felt made of polypropylene (PP) fibers (Fig. 2a) was used as the coating support. Small fabric samples were cut (4 cm × 4 cm) and coated by the solutions previously prepared. After applying the polymer solutions to the PP felt, it was air-dried at room temperature for a minimum of 4 hours (Fig. 2b). Solutions were fairly dispersed on the felt and the amounts deposited were kept constant with respect to the surface area of the felt. The morphology of filtration felts treated with alkylated PEI derivatives was observed by a Hitachi model SU1510 scanning electron microscope (SEM) associated with a Bruker (Quantax) energy dispersive X-ray spectrometer (EDS).

Tissue culture infectious dose 50 ($TCID_{50}$)

CRFK cells were distributed in a 96-well microplate and incubated at 37 °C until reaching a confluent monolayer of in each well. A suspension of feline calicivirus was diluted serially 10-fold, and an aliquot of each dilution was added to the plate (wells without virus served as a control). The plates were incubated at 37 °C for 48 h and observed for 7 days, at which time the number of positive and negative wells was recorded. $TCID_{50}$/mL refers to the number of virus particles per milliliter capable of producing cytopathic effects in 50% of inoculated cells. The results were calculated according to the Reed & Muench method.[35]

Determination of antiviral activity

For textile antiviral activity determination, the protocol used was from international standard ISO 18184 (Second edition 2019(E)).[34] 2 × 2 cm pieces of felt fabric for each sample were put in 50 mL falcon tube, then 0.2 mL of ten folds diluted virus with a $TCID_{50}$ at 10^7 were deposited on the samples for either 30 minutes or 2 hours. Subsequently, the volume of the liquid in each tube was completed using 5 mL of preservation medium (EMEM supplemented with 2% heat-inactivated HS, 1% penicillin G/streptomycin). Several vortex sequences were performed to wash out the virus from the specimen. The eluate of each sample was transferred to the

cell surface of the corresponding wells, with a serial dilution from 1 to 10^7. The microplate was then incubated at 37 °C, in 5% CO_2 and humid atmosphere for at least 5 days. The cytopathic effect of the virus in each sample eluate was observed for each well of the microplate using phase contrast microscope.

To determine antiviral activity of the polymers, the protocol used was the synthetic protocol from the following four documents: Health Canada, Guidance document – Safety and Efficacy Requirements for Hard Surface Disinfectant Drugs (January 2014);[36] American Society for Test Materials (ASTM) E1053-11, Standard test Method to Assess Virucidal Activity of Chemicals Intended for Disinfection of Inanimate, Nonporous Environmental Surface;[38] U.S. Environmental Protection Agency, Office of Chemical Safety and Pollution Prevention, OCSPP 810.2200, Disinfectants for Use on Hard Surfaces-Efficacy Data Recommendations (March 2012)[39] and the International Standard ISO 18184 (Second edition 2019(E)).[34] In summary, for each sample, a volume of 0.5 mL of polymer was placed in a 100 mm × 15 mm glass petri dish, then dried at room temperature, under a hood, overnight before being subjected to testing. A volume of 0.2 mL of the feline calicivirus (ATCC #VR-782), with a $TCID_{50}$ equal to 10^7, was then spread over the dried specimen. Different contact times were observed; or 30 minutes and 2 hours. Assays were carried out in triplicate. The host cells used were also CRFK cells (ATCC #CCL-94).

Calculation of antiviral activity value

Antiviral activity value (M_v) was obtained using the following formula from International Standard ISO 18184.[34]

$$M_v = \log(V_a/V_c) = \log(V_a) - \log(V_c)$$

where M_v is the antiviral activity value; $\log(V_a)$ is the common logarithm average of 3 infectivity titre value immediate after inoculation of the control specimen; $\log(V_c)$ is the common logarithm average of 3 infectivity titre value after 2 hours contacting with the antiviral fabric specimen.

MTT assay for cell viability and proliferation

The MTT assay (thiazolyl blue tetrazolium bromide, M21288, Sigma-Aldrich, Millipore Canada Ltd) is a measure of the metabolic activity of the cells analyzed.[40] The more metabolic activity in the sample, the higher is the signal. In fact, the MTT assay protocol is based on the conversion of water soluble MTT (3-(4,5-dimethylthiazol-2-yl)-2,5-diphenyltetrazolium bromide) compound to an insoluble formazan product. Thereby, only viable cells with active metabolism can convert MTT into formazan. Dead cells lose this ability and therefore show no signal. Thus, the measured absorbance at OD 570 nm is proportional to the number of viable cells.

Cells are cultured in 100 μL of storage medium in a flat-bottomed 96 well plate (tissue culture grade) at a concentration of 500 000 cells per mL and maintained in a 5% CO_2 incubator at 37 °C up to 90% confluent monolayer. The culture medium was then removed and replaced with either the tissue eluate or the polymers and incubated for 4 hours. The appearance of the cells in the different wells was observed using a phase contrast microscope for a qualitative evaluation of the samples' cytotoxicity. Then the MTT reagent was then added (10 μL per well) and the plate was incubated for four hours in the dark at 37 °C, to allow intracellular reduction of the soluble yellow MTT to the insoluble purple formazan dye. Detergent reagent was added to each well to solubilize the formazan dye prior to measuring the absorbance of each sample in a microplate.

Statistical analysis

All results were calculated as the mean ± SEM of independent experiments. Data were analyzed using GraphPad Prism9.1.1 (225) by one-way ANOVA with Dunnett's correction for multiple comparisons. Differences were considered significant at the following P values: *<0.05, **<0.01, ***<0.001, and ****<0.0001.

3. Results and discussion

3.1 Chemical composition of polymers

^{1}H-NMR spectra of PEI and alkylated PEIs are depicted in Fig. 3. The spectrum of branched PEI contains several overlapping peaks between 2–3 ppm corresponding to the methylene protons adjacent to the terminal amine group, which represent a typical ^{1}H-NMR characteristic resonance of branched PEI.[41] After the first modification, resulting from the hexylation step, three significant new broad peaks can be observed at the chemical shift of 0.85, 1.27 and 1.65 ppm.

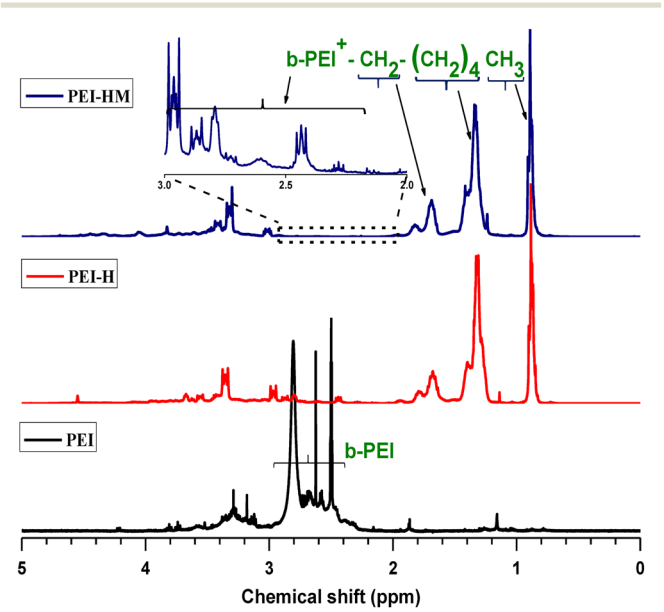

Fig. 3 ^{1}H-NMR spectra of the prepared PEI and alkylated PEI derivatives.

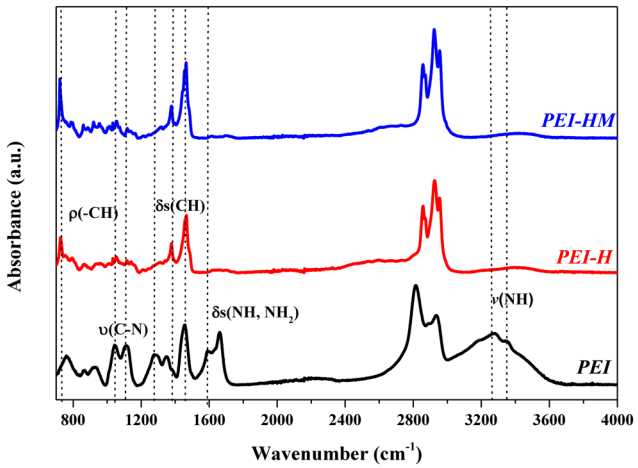

Fig. 4 FTIR spectra of PEI and alkylated PEI derivatives.

The new peaks are, respectively, assigned to the methyl protons of the aliphatic chain (–C**H**$_3$), and two methylene protons of aliphatic chain (N^+–CH_2–(C**H**$_2$)$_4$–CH_3), and (N^+–C**H**$_2$–$(CH_2)_4$–CH_3), thus endorsing the hexylation of the branched PEI.[42] Besides the broadness of the new peaks, no significant difference can be observed between the modified PEI-H and PEI-HM. The above results suggest that a quaternized PEI was successfully synthesized.

FTIR spectroscopy analysis was performed on PEI, PEI-H and PEI-HM (Fig. 4) samples to investigate the degree of alkylation reactions on the PEI's amine functions. The degree of PEI alkylation is mainly evaluated qualitatively by a decrease in the number of vibration bands related to N–H and by an increase in the vibration bands of elongation and deformation of the C–H bonds. FTIR spectrum of PEI without modification exhibits typical characteristic absorption with the presence of primary and secondary amine bands between 3250 to 3400 cm^{-1} due to N–H stretching vibration. Primary amine spectra dispose of two bands (symmetrical and asymmetrical stretches); secondary amine have one, while tertiary amine groups do not absorb in this region of the IR spectrum since they don't contain any N–H bonds.[43,44] The shoulder peak at 3177 cm^{-1} corresponds to the band associated with the synergistic effect between the vibration of the N–H bonds and the O–H vibration of the residual water contained in PEI.[45] The peak at 1591 cm^{-1} refers to the N–H bending vibration of the amine groups found in the polymer structure. The high intensity absorption peak at 1458 cm^{-1} belongs to C–H bending vibration and the shoulder peak characteristic of C–N bond stretching vibration is observed between 1000 and 1350 cm^{-1}. Table S1† summarizes the absorption peaks associated with their corresponding functional group for all polymers.

The IR spectrum of PEI-H shows a reduction in the intensity of the N–H bands vibration in the region of 3250 to 3400 cm^{-1}. The presence of a single band indicates that the primary amines have been alkylated into secondary amines. Moreover, the peaks at 2955, 2858 and 1379 cm^{-1} correspond to the stretching and bending vibrations of the C–H bonds of the aliphatic alkane chains grafted onto the nitrogen. The absorption peak at 720 cm^{-1} is associated to the shearing vibrations of the hexyl C–H bonds. Based on these results one can confirm that the amine functions of PEI-H have been significantly alkylated after the first modification step.

PEI-HM, spectrum presents similar contour as PEI-H with slight variations in intensities (Fig. 4). The absorption peak at 720 cm^{-1} (C–H) and 1460 cm^{-1} (N–H + CH_2 scissors) slightly intense compared to PEI-H, which could be explained by a higher grafting amount of alkyl chains on the amine groups of PEI-HM and then by a higher degree of alkylation.

The elemental composition and the alkylation reactions degree of PEI and modified PEIs were evaluated by XPS. Fig. 5a depicts the survey spectrum of PEI, PEI-H, and PEI-HM with the presence of C and N as the main elements in addition to O, I, and Br. Fig. 5b shows of N 1s/C 1s ratio of unmodified PEI, PEI-H, and PEI-HM after the first and second modifications, respectively. The (N/C) ratio from the survey is 0.40 while the theoretical ratio is 0.46. The difference between the theoretical and experimental values was mainly due to organic surface contamination by silicon, chloride, and oxygen. The significant decrease in N/C observed after PEI modification can be attributed to the alkylation on the PEI, in agreement with NMR and FTIR results indicating a significant enhancement of the carbon structure in the polymer coating. Furthermore, the second modification step led to higher alkylation degree of the polymer.

For a detailed analysis of PEI, the high-resolution spectra N 1s (Fig. 5c–e), and C 1s (ESI† data, Fig. S1) were fitted. The N 1s spectrum was decomposed into 2 components for the unmodified PEI attributed to –NH_2 at 399.2 eV and C–N– at 400.3 eV which are typical characteristics of standard PEI.[46] After the PEI modification, the PEI-H is composed of an additional third component attributed to the quaternary ammonium peak –N^+ at 402.0 eV, demonstrating a highly positively charged polymer. Furthermore, the second step modification led to a higher concentration amount of –N^+.[47]

The relative proportion of N 1s peak of –NH_2 component significantly decreases after PEI first step modification giving rise to quaternary ammonium –N^+ which indicates a high degree of alkylation of the polymer coating. The second step modification results even in a higher alkylation amount with over 80% of N 1s peak attributed to –N^+. Table 1 summarizes the N 1s peak components binding energy and relative proportions.

3.2 Surface morphology and EDS elemental composition of the polymeric coatings

The morphology of untreated and treated felts was investigated using SEM coupled with EDS analysis. Fig. 6a represents the image of the native uncoated filtration felt displaying a very smooth surface of PP fibers. Fig. 6b shows

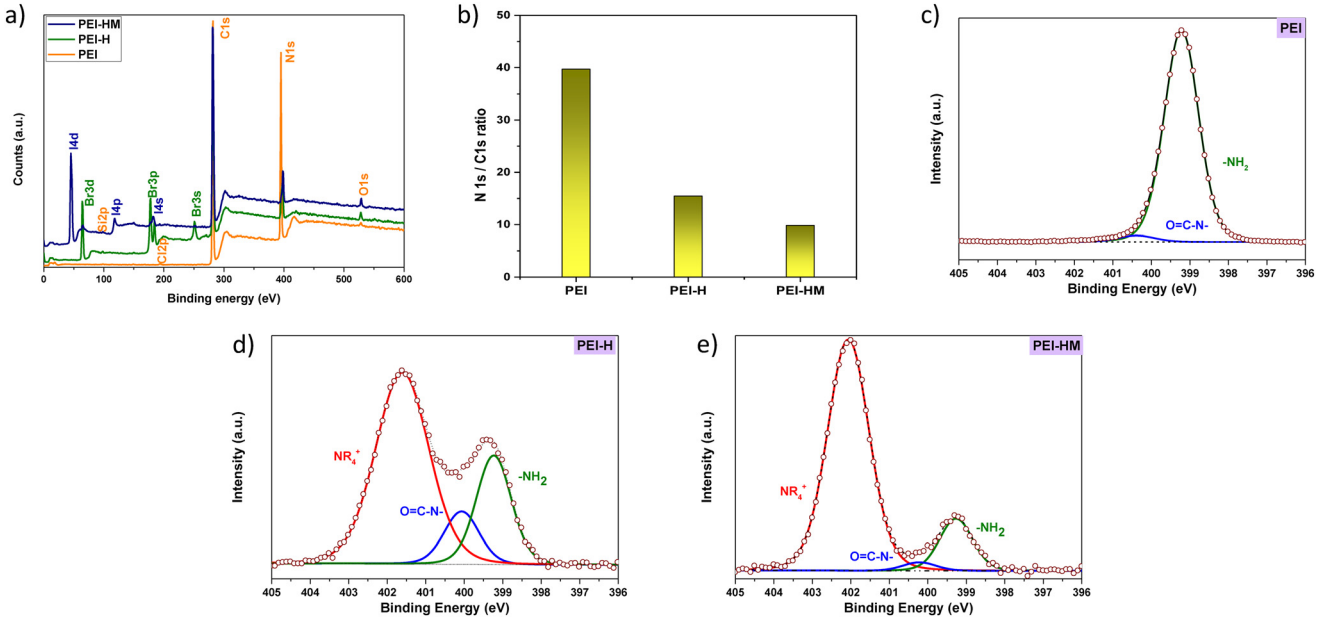

Fig. 5 (a) XPS survey of PEI and alkylated PEI derivatives, (b) N 1s/C 1s atomic ratio for PEI, PEI-H and PEI-HM, (c)–(e) the high-resolution XPS N 1s spectra of PEI, PEI-H and PEI-HM, respectively.

the felt after being treated with a solution of PEI at a concentration of 1.0 μmol N per cm^2. Below this polymer concentration, the coating was relatively imperceptible. PEI is fairly dispersed on the felt's surface and between the fibers without agglomeration. At 1.0 μmol N per cm^2, the polymeric coating is visible and appears to be paler on the fibers. Fig. 5c shows the coating at 1000× magnification.

EDS mapping of PEI and PEI derivatives was performed, and the concentration (at%) of the main elements C, N, O, Br, and I are summarized in Table 2. The elemental composition of PEI is C (78.0%), N (17.0%) and O (4.6%). The presence of oxygen is due to the residual water in the polymer after drying. As mentioned above, the amount was estimated to be around 3% by measuring the mass after drying. The hexylated PEI contains C (87.5%) and N (6.8%). The increase in carbon and the decrease in nitrogen are explained by the addition of carbon chains to the structure. PEI-H also contains Br (6.0%) which corresponds approximately to the percentage value of nitrogen detected. According to FTIR and XPS experiments, the presence of quaternary ammonium implies that the amount of bromide anion should be equivalent to the amount of quaternary ammonium nitrogen. The equivalence therefore likely means that all the amine functions have been quaternized after the first alkylation step. The absence of bromine confirms that dialyzes have been well carried out and that there is no residual 1-bromohexane reagent. PEI-HM contains C (82.2%), N (7.4%), O (2.8%), Br (0.2%) and I (7.5%). Based on these results, the amount of iodine which is supposed to be the counter anion of the $-N^+$ group is equivalent to the nitrogen atomic percentage. EDS mapping images are reported in the ESI† (Fig. S2).

Table 1 N 1s fitting results of PEI and alkylated PEI derivatives

Polymer coating	$-NH_2$	N–C	$-N^+$
	Concentration (%)		
PEI	96.9	3.1	—
PEI-H	24.1	11.6	64.3
PEI-HM	14.8	2.4	82.8

3.3 Antiviral activity and biocompatibility of coated PP fabrics

PEI and alkylated PEI derivatives coated felts were tested against FCV to study the virucidal efficiency. According to the International Standard ISO 18184:2019, the antiviral activity value (M_v), which represents the log reduction (V_a/V_c), is considered to be a good antiviral activity when $M_v \geq 3$.[34] It corresponds to an inactivation rate of ≥99.9% when comparing tests between the biocide and the virus control.

The efficiency of FCV viral inactivation of PP felt coated with PEI, PEI-H and PEI-HM at a concentration of 1×10^{-4} μmol N per cm^2, after 4 hours of exposure, is presented at Fig. 7a. The results show that the uncoated PP fabric has a reduction of 3 log in the viral titer and when PP felt is coated with PEI and alkylated-PEI coatings, the antiviral activity values considerably increased. In contrast with other works, PEI-HM ($M_v \geq 4$) does not have the higher antiviral efficiency among the different coatings of polymers.[48] The decrease in the number of viruses for PEI-HM coating is rather good but it is still less efficient that PEI and hexylated PEI activity value of $M_v \geq 6$ (99.9999%). From the above results, one can note that an additional modification of PEI after the initial alkylation does not necessary contribute to higher antiviral

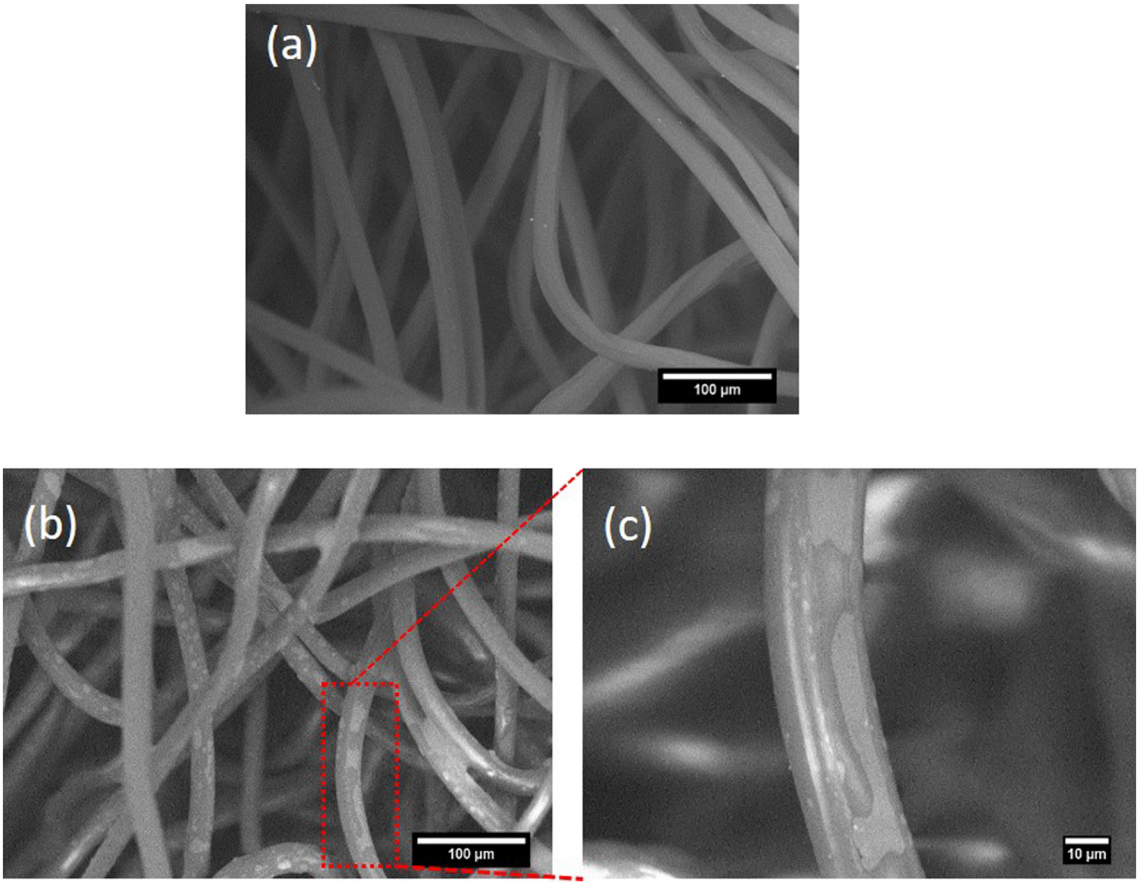

Fig. 6 SEM images of (a) uncoated PP felt, (b) PP felt coated with PEI at 1.0 µmol N per cm^2 (×250) and (c) PP felt coated with PEI at 1.0 µmol N per cm^2 (×1000).

activity of the coating, emphasizing that a higher N^+ charge density is not necessarily correlated to a higher antiviral activity. The logarithmic reduction value also does not change as a function of the concentration in µmol N per cm^2 for each polymer (ESI† data, Table S3). Furthermore, it is possible that the high antiviral activity of PEI on PP felt was related to amino functions that protonate on PEI structure. In the antiviral activity assay, PEI/PP is in contact with the preservation medium (EMEM supplemented with 2% heat-inactivated HS, 1% penicillin G/streptomycin). This cell culture medium has a physiological pH of 7.0 to 7.4.[49] Primary amine functions have a relatively high pK_a, so that at physiological pH, amino groups tend to bind a proton and become positively charged (NH_3^+).

Our approach stands out by studying the effect of different concentrations of polymers on antiviral activity,[28,50] while most articles report antiviral efficiency of *N*-alkylated-PEI derivatives as a function of the length of alkyl chains grafted onto the PEI or compare antiviral properties of PEI to other polymers at a single concentration. The difference between the strong virucidal effect of PEI against FCV and the less efficient results published in literature may be explained by the type of virus used in the experiment but also by the concentration of PEI coating on the filtration felt. Calais *et al.* did a similar experiment and coated a PP mask fabric with a 0.25% (w/v) branched PEI-750 kDa solution and obtained a less significant reduced viral titer of ≥99.99% against MHV-3 virus.[51] The virucidal activity of PEI can be modulated by the concentration deposited on the filtration felt. Therefore, the filtration felt presents a higher antiviral efficiency at lower concentrations of PEI.[52]

Table 2 Elemental composition obtained from semi-quantitative EDS analysis for PEI, PEI-H and PEI-HM

	Elemental composition (at%)				
Polymers	C	N	O	Br	I
PEI	78.0	17.0	4.6	—	—
PEI-H	85.7	6.8	1.6	6.0	—
PEI-HM	82.2	7.4	2.8	0.2	7.5

MTT assay was used to investigate the *in vitro* cytotoxicity of PP filtration felt coated with PEI-HM which is most likely to be cytotoxic due to its higher amount of quaternary ammonium functions compared to PEI and PEI-H. Polymers with high charge density and molecular weight have been reported to exhibit higher cytotoxicity.[53] Cell viability of CRFK after 4 hours of incubation with PP felt coated with PEI-HM dissolved in a solution of water and 2-propanol (40/60% v/v) at five concentrations (1; 1×10^{-1}; 1×10^{-2}; 1×10^{-3} and 1 ×

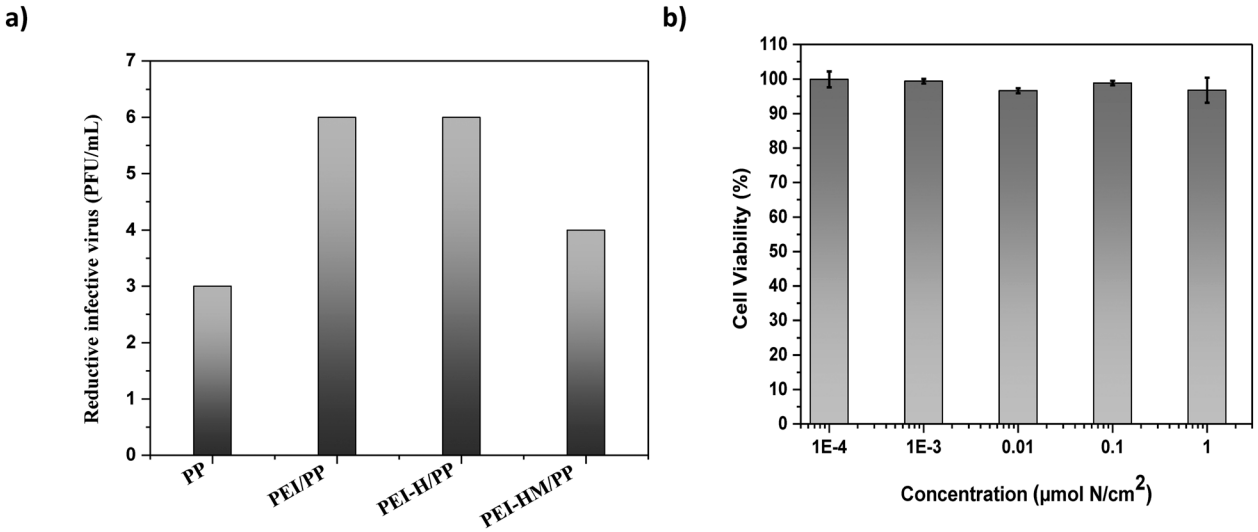

Fig. 7 a) Reduced viral titer of FCV after 4 hours incubation with uncoated PP and PP felt coated with PEI, PEI-H, and PEI-HM at a concentration of 1×10^{-4} μmol N per cm^2 (the error bar is too small to display), and b) cell viability of CFRK cells after 4 hours of incubation with PP felt coated with PEI-HM at different concentrations (tests were conducted in triplicate).

10^{-4} μmol N per cm^2) was determined. None of these concentrations of coating presents significant cytotoxicity to CRFK cells (Fig. 7b) as proved by the high cell viability of ≥95%. This suggests that at these concentrations, PEI and PEI-H are not cytotoxic as well.

Table 3 reports a summary of different studies on the antiviral activity of PEIs and PEI-based compounds. The latter were tested against different viruses at different concentrations. The antiviral efficiency of PP felt coated at 1×10^{-4} μmol N per cm^2 against FCV in the present study is found to be highly superior to all the compounds listed in Table 3. Considering the excellent antiviral activity, PEI used at this level of concentration can be expected to be tested against other viruses and could exhibit a strong virucidal character. Commercial PEI coatings provide a promising, attractive, and inexpensive method to annihilate viruses.

Table 3 Summary of antiviral activity of various PEI compounds from the literature

Compounds	Concentration of PEI for the antiviral activity evaluation	Viruses	Antiviral activity		Ref.
			Titer reduction log	% reduction	
Branched PEI-750 kDa	—	*Escherichia coli* bacteriophage MS2	≥4	≥99.99%	54
Branched PEI-25 kDa	—	*Escherichia coli* bacteriophage T4	5	99.999%	55
Linear PEI-25 kDa	52 nM	Human papillomaviruses (HPV16)	>2	>99%	50
PEI aqueous solutions at 10, 1.0 and 0.1 mg mL^{-1}	—	SARS-CoV-2	PEI aqueous solutions: 0%	PEI aqueous solutions: 0%	56
AgNPs–PEI			AgNPs–PEI on PP: 3	AgNPs–PEI on PP: 99.9%	
PEI	—	Murine hepatitis virus (MHV-3)	PEI: 4	PEI: 99.99%	51
PEI/Cu^{2+}			PEI/Cu^{2+}: 5	PEI/Cu^{2+}: 99.999%	
PEI	—	Influenza A (H1N1)	PEI: inactive for both viruses	PEI: inactive for both viruses 0%	48
N,*N*-Hexyl,methyl-PEI		Influenza A (H3N2)	H1N1/*N*,*N*-hexyl,methyl-PEI: 3	H1N1/*N*,*N*-hexyl,methyl-PEI: 99.9%	
N,*N*-Hexyl,methyl-PEI	3.47 μg mm^{-2}	Influenza A (H1N1)	4.5 ± 0.3	≥99.99%	57
N,*N*-Dodecyl,methyl-PEI	320 μg mm^{-2}	Herpes simplex viruses (HSV-1 and 2)	HSV-1: 5 HSV-2: 4	HSV-1: 99.999% HSV-2: 99.99%	58
N,*N*-Dodecyl,methyl-PEI	—	Influenza A (H1N1)	4	99.99%	25
N,*N*-Dodecyl,methyl-PEI	—	Influenza A (H3N2)	H3N2: >3.5	H3N2: >99.9%	59
		Influenza A (H4N2)	H4N2: >4.5	H4N2: >99.99%	
Branched PEI-750 kDa	1×10^{-4} μmol N per cm^2	FCV	PEI: 6	PEI: 99.9999%	This study
PEI-H			PEI-H: 6	PEI-H: 99.9999%	

4. Conclusions

This study investigated the antiviral activity of a filtration felt made of polypropylene fibers coated with PEI and alkylated PEI derivatives at different concentrations. The results showed that PEI and PEI-H coated PP have a stronger antiviral efficiency than uncoated PP and PEI-HM coating with ≥99.9999% reduced viral titer against feline calicivirus (FCV). Thus, this work demonstrated with this one-step low-cost process that a PP felt coated with PEI is a promising material for the development of protective masks, textiles and building air filtration systems with highly effective antiviral properties. A further approach on the development of immobilized PEI-coated polymer fabrics and hard surfaces with strong biocide properties and non-cytotoxic effect would be of interest for many medical applications.

Data availability

The data supporting this article have been included as part of the ESI.†

Conflicts of interest

The authors declare that they have no known competing financial interests or personal relationships that could have appeared to influence the work reported in this article.

Acknowledgements

The financial support of the Natural Sciences and Engineering Research Council of Canada (NSERC) is gratefully acknowledged for funding this work. The authors would also like to thank Julie Alain (COALIA) for the SEM measurements, Pierre Audet (Université Laval) for his expertise in NMR, Sonia Blais (Université de Sherbrooke) for her technical contribution to XPS experiments and Vanessa Leblond-Drolet for her implication in the biological assays. A special thank you to Lambert Gagné, Laura Brière and Marianne Tousignant for their technical contribution.

References

1 World Health Organization (WHO) - Coronavirus (COVID-19) Dashboard, **https://covid19.who.int** (accessed March 9, 2023).
2 M.-M. Zhu, Y. Fang, Y.-C. Chen, Y.-Q. Lei, L.-F. Fang, B.-K. Zhu and H. Matsuyama, Antifouling and antibacterial behavior of membranes containing quaternary ammonium and zwitterionic polymers, *J. Colloid Interface Sci.*, 2021, **584**, 225–235, DOI: **10.1016/j.jcis.2020.09.041**.
3 H. Zhang, S. Zhao, A. Li, K. Bian, S. Shen, M. Tao and P. Shi, Structure-dependent antimicrobial mechanism of quaternary ammonium resins and a novel synthesis of highly efficient antimicrobial resin, *Sci. Total Environ.*, 2021, **768**, 144450, DOI: **10.1016/j.scitotenv.2020.144450**.
4 A. Palantoken, M. S. Yilmaz, M. A. Yapaöz, E. Y. Tulunay, T. Eren and S. Piskin, Dual antimicrobial effects induced by hydrogel incorporated with UV-curable quaternary ammonium polyethyleneimine and AgNO3, *Mater. Sci. Eng., C*, 2016, **68**, 494–504, DOI: **10.1016/j.msec.2016.06.005**.
5 N. Beyth, S. Farah, A. J. Domb and E. I. Weiss, Antibacterial dental resin composites, *React. Funct. Polym.*, 2014, **75**, 81–88, DOI: **10.1016/j.reactfunctpolym.2013.11.011**.
6 A. M. Klibanov, Permanently microbicidal materials coatings, *J. Mater. Chem.*, 2007, **17**(24), 2479–2482, DOI: **10.1039/B702079A**.
7 A. D. Fuchs and J. C. Tiller, Contact-Active Antimicrobial Coatings Derived from Aqueous Suspensions, *Angew. Chem., Int. Ed.*, 2006, **45**(40), 6759–6762, DOI: **10.1002/anie.200602738**.
8 N.-N. Vu, C. Venne, S. Ladhari, A. Saidi, L. Moskovchenko, T. T. Lai, Y. Xiao, S. Barnabe, B. Barbeau and P. Nguyen-Tri, Rapid Assessment of Biological Activity of Ag-Based Antiviral Coatings for the Treatment of Textile Fabrics Used in Protective Equipment Against Coronavirus, *ACS Appl. Bio Mater.*, 2022, **5**(7), 3405–3417, DOI: **10.1021/acsabm.2c00360**.
9 M. M. Garcia, B. L. da Silva, R. Sorrechia, R. C. L. R. Pietro and L. A. Chiavacci, Sustainable Antibacterial Activity of Polyamide Fabrics Containing ZnO Nanoparticles, *ACS Appl. Bio Mater.*, 2022, **5**(8), 3667–3677, DOI: **10.1021/acsabm.2c00104**.
10 Á. Serrano-Aroca, M. Ferrandis-Montesinos and R. Wang, Antiviral Properties of Alginate-Based Biomaterials: Promising Antiviral Agents against SARS-CoV-2, *ACS Appl. Bio Mater.*, 2021, **4**(8), 5897–5907, DOI: **10.1021/acsabm.1c00523**.
11 G. Matafonova and V. Batoev, Dual-wavelength light radiation for synergistic water disinfection, *Sci. Total Environ.*, 2022, **806**, 151233, DOI: **10.1016/j.scitotenv.2021.151233**.
12 H. Zhang, A. Li, K. Bian, S. Shen and P. Shi, Surficial N+ charge density indicating antibacterial capacity of quaternary ammonium resins in water environment, *PLoS One*, 2020, **15**(9), e0239941, DOI: **10.1371/journal.pone.0239941**.
13 I. Yudovin-Farber, J. Golenser, N. Beyth, E. I. Weiss and A. J. Domb, Quaternary Ammonium Polyethyleneimine: Antibacterial Activity, *J. Nanomater.*, 2010, **2010**, 826343, DOI: **10.1155/2010/826343**.
14 W. Jaeger, J. Bohrisch and A. Laschewsky, Synthetic polymers with quaternary nitrogen atoms—Synthesis and structure of the most used type of cationic polyelectrolytes, *Prog. Polym. Sci.*, 2010, **35**(5), 511–577, DOI: **10.1016/j.progpolymsci.2010.01.002**.
15 C. Wang, X. Wang, L. Du, Y. Dong, B. Hu, J. Zhou, Y. Shi, S. Bai, Y. Huang and H. Cao, *et al.* Harnessing pH-Sensitive Polycation Vehicles for the Efficient siRNA Delivery, *ACS Appl. Mater. Interfaces*, 2021, **13**(2), 2218–2229, DOI: **10.1021/acsami.0c17866**.
16 A. Mondrzyk, J. Fischer and H. Ritter, Antibacterial materials: structure–bioactivity relationship of epoxy–amine resins containing quaternary ammonium compounds

covalently attached, *Polym. Int.*, 2014, **63**(7), 1192–1196, DOI: **10.1002/pi.4690**.

17 K. A. Gibney, I. Sovadinova, A. I. Lopez, M. Urban, Z. Ridgway, G. A. Caputo and K. Kuroda, Poly(ethylene imine)s as antimicrobial agents with selective activity, *Macromol. Biosci.*, 2012, **12**(9), 1279–1289, DOI: **10.1002/mabi.201200052**.

18 Y. Zhao, Y. Qian, H. Wang, W. Zhao, J. Zhao and H. Zhang, Bioinspired Polycation Functionalization of the Polyurethane Surface for Enhanced Lubrication, Antibacterial Property, and Anticoagulation, *ACS Appl. Polym. Mater.*, 2023, **5**(6), 3999–4010, DOI: **10.1021/acsapm.3c00234**.

19 C. Wang, O. Y. Zolotarskaya, S. S. Nair, C. J. Ehrhardt, D. E. Ohman, K. J. Wynne and V. K. Yadavalli, Real-Time Observation of Antimicrobial Polycation Effects on Escherichia coli: Adapting the Carpet Model for Membrane Disruption to Quaternary Copolyoxetanes, *Langmuir*, 2016, **32**(12), 2975–2984, DOI: **10.1021/acs.langmuir.5b04247**.

20 S. Kumaran, E. Oh, S. Han and H. J. Choi, Photopolymerizable, Universal Antimicrobial Coating to Produce High-Performing, Multifunctional Face Masks, *Nano Lett.*, 2021, **21**(12), 5422–5429, DOI: **10.1021/acs.nanolett.1c00525**.

21 M. Sorci, T. D. Fink, V. Sharma, S. Singh, R. Chen, B. L. Arduini, K. Dovidenko, C. L. Heldt, E. F. Palermo and R. H. Zha, Virucidal N95 Respirator Face Masks via Ultrathin Surface-Grafted Quaternary Ammonium Polymer Coatings, *ACS Appl. Mater. Interfaces*, 2022, **14**(22), 25135–25146, DOI: **10.1021/acsami.2c04165**.

22 R. Hirao, H. Takeuchi, J. Kawada and N. Ishida, Polypropylene-Rendered Antiviral by Three-Dimensionally Surface-Grafted Poly(N-benzyl-4-vinylpyridinium bromide), *ACS Appl. Mater. Interfaces*, 2024, **16**(8), 10590–10600, DOI: **10.1021/acsami.3c15125**.

23 L. A. T. W. Asri, M. Crismaru, S. Roest, Y. Chen, O. Ivashenko, P. Rudolf, J. C. Tiller, H. C. van der Mei, T. J. A. Loontjens and H. J. Busscher, A Shape-Adaptive, Antibacterial-Coating of Immobilized Quaternary-Ammonium Compounds Tethered on Hyperbranched Polyurea and its Mechanism of Action, *Adv. Funct. Mater.*, 2014, **24**(3), 346–355, DOI: **10.1002/adfm.201301686**.

24 A. Bhatti and R. K. DeLong, Nanoscale Interaction Mechanisms of Antiviral Activity, *ACS Pharmacol. Transl. Sci.*, 2023, **6**(2), 220–228, DOI: **10.1021/acsptsci.2c00195**.

25 J. Haldar, D. An, L. A. de Cienguegos, J. Chen and A. M. Klibanov, Polymeric coatings that inactivate viruses and bacteria, *US Pat.*, US20100136072A1, 2010.

26 J. Haldar, D. An, L. Á. de Cienfuegos, J. Chen and A. M. Klibanov, Polymeric coatings that inactivate both influenza virus and pathogenic bacteria, *Proc. Natl. Acad. Sci. U. S. A.*, 2006, **103**(47), 17667–17671, DOI: **10.1073/pnas.0608803103**.

27 I. F. Tsao, H. Y. Wang and C. Shipman Jr, Interaction of infectious viral particles with a quaternary ammonium chlorid (QAC) surface, *Biotechnol. Bioeng.*, 1989, **34**(5), 639–646, DOI: **10.1002/bit.260340508**.

28 D. Park, J. Wang and A. M. Klibanov, One-Step, Painting-Like Coating Procedures To Make Surfaces Highly and Permanently Bactericidal, *Biotechnol. Prog.*, 2006, **22**(2), 584–589, DOI: **10.1021/bp0503383**.

29 A. P. Mouritz, J. Galos, D. P. Linklater, R. B. Ladani, E. Kandare, R. J. Crawford and E. P. Ivanova, Towards antiviral polymer composites to combat COVID-19 transmission, *Nano Sel.*, 2021, **2**(11), 2061–2071, DOI: **10.1002/nano.202100078**.

30 L. Ouyang, N. Wang, J. Irudayaraj and T. Majima, Virus on surfaces: Chemical mechanism, influence factors, disinfection strategies, and implications for virus repelling surface design, *Adv. Colloid Interface Sci.*, 2023, **320**, 103006, DOI: **10.1016/j.cis.2023.103006**.

31 S. Mohapatra, L. Yutao, S. G. Goh, C. Ng, Y. Luhua, N. H. Tran and K. Y.-H. Gin, Quaternary ammonium compounds of emerging concern: Classification, occurrence, fate, toxicity and antimicrobial resistance, *J. Hazard. Mater.*, 2023, **445**, 130393, DOI: **10.1016/j.jhazmat.2022.130393**.

32 B. B. Hsu, S. Y. Wong, P. T. Hammond, J. Chen and A. M. Klibanov, Mechanism of inactivation of influenza viruses by immobilized hydrophobic polycations, *Proc. Natl. Acad. Sci. U. S. A.*, 2011, **108**(1), 61–66, DOI: **10.1073/pnas.1017012108**.

33 J. Haldar, A. K. Weight and A. M. Klibanov, Preparation, application and testing of permanent antibacterial and antiviral coatings, *Nat. Protoc.*, 2007, **2**(10), 2412–2417, DOI: **10.1038/nprot.2007.353**.

34 International Organization for Standardization, *ISO 18184:2019 Textiles – Determination of antiviral activity of textile products*, 2nd edn, 2019.

35 L. J. Reed and H. Muench, A Simple Method of Estimating Fifty per Cent Endpoints, *Am. J. Epidemiol.*, 1938, **27**(3), 493–497, DOI: **10.1093/oxfordjournals.aje.a118408**.

36 Health Canada, *Guidance Document – Safety and efficacy requirements for hard surface disinfectant drugs*, January 2014 (see the website: **https://www.canada.ca/content/dam/hc-sc/migration/hc-sc/dhp-mps/alt_formats/pdf/prodpharma/applic-demande/guide-ld/disinfect-desinfect/hard-surface-surfaces-dures-eng.pdf**).

37 G. Beamson and D. Briggs, *High Resolution XPS of Organic Polymers, The Scienta ESCA300 Database*, John Wiley & Sons, Chichester, 1992, ISBN 0471 935921.

38 ASTM, *E1053-11 – Standard test Method to Assess Virucidal Activity of Chemicals Intended for Disinfection of Inanimate, Nonporous Environmental surface*, 2020.

39 This document was obtained from United States Environmental Protection of Agency (EPA), OCSPP 810.2200: Disinfectants for use on environmental surfaces - Guidance for Efficacy Testing, 2018.

40 P. Kumar, A. Nagarajan and P. D. Uchil, Analysis of Cell Viability by the MTT Assay, *Cold Spring Harb. Protoc.*, 2018, (6), DOI: **10.1101/pdb.prot095505**.

41 D. R. Holycross and M. Chai, Comprehensive NMR Studies of the Structures and Properties of PEI Polymers, *Macromolecules*, 2013, **46**(17), 6891–6897, DOI: **10.1021/ma4011796**.

42 X. Xu, H. Xiao, Z. Ziaee, H. Wang, Y. Guan and A. Zheng, Novel comb-like ionenes with aliphatic side chains:

synthesis and antimicrobial properties, *J. Mater. Sci.*, 2013, **48**(3), 1162–1171, DOI: **10.1007/s10853-012-6854-8**.

43 D. L. Pavia, G. M. Lampman and G. S. J. Kriz, *Introduction to Spectroscopy: A Guide for Students of Organic Chemistry*, 1979.

44 E. Pretsch, J. Seibl, W. Simon and T. Clerc, *Tables of Spectral Data for Structure Determination of Organic Compounds*, 1989.

45 B. Chen, D. Chen and X. Zhao, Radioactive wastewater treatment with modified aromatic polyamide reverse osmosis membranes via quaternary ammonium cation grafting, *Sep. Purif. Technol.*, 2020, **252**, 117378, DOI: **10.1016/j.seppur.2020.117378**.

46 K. Gu, S. Pang, B. Yang, Y. Ji, Y. Zhou and C. Gao, Polyethyleneimine/4,4′-Bis(chloromethyl)-1,1′-biphenyl nanofiltration membrane for metal ions removal in acid wastewater, *J. Membr. Sci.*, 2020, **614**, 118497, DOI: **10.1016/j.memsci.2020.118497**.

47 X. Liang, B. Liang, J. Wei, S. Zhong, R. Zhang, Y. Yin, Y. Zhang, H. Hu and Z. Huang, A cellulose-based adsorbent with pendant groups of quaternary ammonium and amino for enhanced capture of aqueous Cr(VI), *Int. J. Biol. Macromol.*, 2020, **148**, 802–810, DOI: **10.1016/j.ijbiomac.2020.01.184**.

48 H. Liu, I. Elkin, J. Chen and A. M. Klibanov, Why do Some Immobilized N-Alkylated Polyethylenimines Far Surpass Others in Inactivating Influenza Viruses?, *Biomacromolecules*, 2014, **16**(1), 351–356, DOI: **10.1021/bm5015427**.

49 ATCC, *Eagle's Minimum Essential Medium (EMEM), Quality control specifications*, (accessed June 5, 2024).

50 G. A. Spoden, K. Besold, S. Krauter, B. Plachter, N. Hanik, A. F. Kilbinger, C. Lambert and L. Florin, Polyethylenimine is a strong inhibitor of human papillomavirus and cytomegalovirus infection, *Antimicrob. Agents Chemother.*, 2012, **56**(1), 75–82, DOI: **10.1128/aac.05147-11**.

51 G. B. Calais, J. B. M. R. Neto, R. A. Bataglioli, P. Chevalier, J. Tsukamoto, C. W. Arns, D. Mantovani and M. M. Beppu, Bioactive textile coatings for improved viral protection: A study of polypropylene masks coated with copper salt and organic antimicrobial agents, *Appl. Surf. Sci.*, 2023, **638**, 158112, DOI: **10.1016/j.apsusc.2023.158112**.

52 N. Jarach, H. Dodiuk and S. Kenig, Polymers in the Medical Antiviral Front-Line, in *Polymers*, 2020, vol. 12.

53 S. Jain, S. Kumar, A. K. Agrawal, K. Thanki and U. C. Banerjee, Enhanced Transfection Efficiency and Reduced Cytotoxicity of Novel Lipid–Polymer Hybrid Nanoplexes, *Mol. Pharmaceutics*, 2013, **10**(6), 2416–2425, DOI: **10.1021/mp400036w**.

54 T. R. Sinclair, D. Robles, B. Raza, S. van den Hengel, S. A. Rutjes, A. M. de Roda Husman, J. de Grooth, W. M. de Vos and H. D. W. Roesink, Virus reduction through microfiltration membranes modified with a cationic polymer for drinking water applications, *Colloids Surf., A*, 2018, **551**, 33–41, DOI: **10.1016/j.colsurfa.2018.04.056**.

55 G. Tiliket, D. L. Sage, V. Moules, M. Rosa-Calatrava, B. Lina, J. M. Valleton, Q. T. Nguyen and L. Lebrun, A new material for airborne virus filtration, *Chem. Eng. J.*, 2011, **173**(2), 341–351, DOI: **10.1016/j.cej.2011.07.059**.

56 M. Baselga, I. Uranga-Murillo, D. de Miguel, M. Arias, V. Sebastián, J. Pardo and M. Arruebo, Silver Nanoparticles–Polyethyleneimine-Based Coatings with Antiviral Activity against SARS-CoV-2: A New Method to Functionalize Filtration Media, in *Materials*, 2022, vol. 15.

57 H. Liu, Y. Kim, K. Mello, J. Lovaasen, A. Shah, N. Rice, J. H. Yim, D. Pappas and A. M. Klibanov, Aerosol-assisted plasma deposition of hydrophobic polycations makes surfaces highly antimicrobial, *Appl. Biochem. Biotechnol.*, 2014, **172**(3), 1254–1264, DOI: **10.1007/s12010-013-0593-4**.

58 A. M. Larson, H. S. Oh, D. M. Knipe and A. M. Klibanov, Decreasing herpes simplex viral infectivity in solution by surface-immobilized and suspended N,N-dodecyl,methyl-polyethylenimine, *Pharm. Res.*, 2013, **30**(1), 25–31, DOI: **10.1007/s11095-012-0825-2**.

59 J. Haldar, J. Chen, T. M. Tumpey, L. V. Gubareva and A. M. Klibanov, Hydrophobic polycationic coatings inactivate wild-type and zanamivir- and/or oseltamivir-resistant human and avian influenza viruses, *Biotechnol. Lett.*, 2008, **30**(3), 475–479, DOI: **10.1007/s10529-007-9565-5**.